A combined theoretical and experimental study on the oxidation of fulvic acid by the sulfate radical anion†

Pedro M. David Gara,[a] Gabriela N. Bosio,[a] Mónica C. Gonzalez,[a] Nino Russo,*[b] Maria del Carmen Michelini,[b] Reinaldo Pis Diez[c] and Daniel O. Mártire*[a]

Received 16th January 2009, Accepted 14th May 2009
First published as an Advance Article on the web 27th May 2009
DOI: 10.1039/b900961b

The kinetics of the reaction of sulfate radicals with the IHSS Waskish peat fulvic acid in water was investigated in the temperature range from 289.2 to 305.2 K. The proposed mechanism considers the reversible binding of the sulfate radicals by the fulvic acid. The kinetic analysis of the data allows the determination of the thermodynamic parameters $\Delta G^\circ = -10.2$ kcal mol^{-1}, $\Delta H^\circ = -16$ kcal mol^{-1} and $\Delta S^\circ = -20.3$ cal K^{-1} mol^{-1} for the reversible association at 298.2 K. Theoretical (DFT) calculations performed with the Buffle model of the fulvic acids support the formation of H-bonded adducts between the inorganic radicals and the humic substances. The experimental enthalpy change compares well with the theoretical values found for some of the investigated adducts.

Introduction

Humic acids (HA) and fulvic acids (FA), which are a mixture of the decomposition products of plant and animal residues, are the main components of natural organic matter (NOM) and can be found most commonly in soil, natural water and sediments. The presence of NOM in raw water could affect the water quality during the water purification process. For example, disinfection by-products like trihalomethanes (THMs), can be formed from chlorination in drinking water containing NOM.[1,2] In some surface waters over 70% of NOM was assigned to FA.[3] FA are difficult to remove by the conventional treatment processes, such as coagulation and sedimentation.[4]

In situ chemical oxidation (ISCO) involves the introduction of an oxidant into the subsurface for the purpose of transforming ground-water or soil contaminants into less harmful chemical species. There are several chemicals that have been used for ISCO; however, the most commonly used oxidants are: permanganate, hydrogen peroxide and iron, peroxodisulfate, and ozone. Peroxodisulfate oxidation is generally carried out under heat-, photo-, acid-, base- or metal-activated conditions because oxidation rates can be greatly accelerated, resulting from the formation of a variety of free radical species.[5] The costs of organic-waste destruction are higher for heavily chlorinated wastes and for waste containing substantial amount of non-hazardous organics, such as HA and FA in contaminated soils. These effects are expected to be related to the $SO_4^{\bullet-}$ scavenging by humic substances (HS). To model the effect of NOM during water treatments involving peroxodisulfate, kinetic data on the $SO_4^{\bullet-}$-mediated oxidation of NOM is necessary.

In a previous paper we reported that the kinetics of the aqueous phase reaction of sulfate radicals with HS of different origin can be interpreted in terms of a mechanism which in a first step considers the reversible binding of the sulfate radicals by the humic substances.[6] Also, we have recently performed a mechanistic investigation of the reaction of the sulfate radical with gallic acid.[7] In that work we have used gallic acid as a low molecular weight model of HS. The flash-photolysis experiments performed with this system showed: (a) linear plots of the apparent decay rate constant of the sulfate radicals *vs.* the molar concentration of gallic acid, and (b) the formation of phenoxyl radicals of the organic substrate as reaction intermediates. The DFT calculations confirmed the experimental results and supported the H-abstraction by the sulfate radical from gallic acid. To gain further information on the effect of the lighter molecular weight HS components, we employ here the flash-photolysis technique to investigate the kinetics of the reaction of the sulfate radicals with FA.

We also perform theoretical calculations employing the Buffle model of FA to explain the chemical nature of the interaction between the sulfate radicals and FA.[8] Two theoretical works involving FA models and their interaction with metal ions have been carried out elsewhere. Nantsis and Carper investigated the formation and hydration of 2 : 1 complexes of a model of FA with Mg^{2+} and Cd^{2+}, Zn^{2+} or Pb^{2+} by means of semiempirical PM3 calculations.[9] Those authors provide some thermodynamic properties of both hydrated and unhydrated complexes as well as a description of hydrogen bonding features. On the other hand, de Castro Ramalho and coworkers compare the relative stability and hydration behavior of a FA model with Cd^{2+} and Zn^{2+}.[10] Those authors use NVT molecular dynamics simulations to generate configurations, which are further subject to an NBO analysis within the framework of DFT. We would like to stress that none of those previous works include geometry optimizations at the DFT level.

[a]*Instituto de Investigaciones Fisicoquímicas Teóricas y Aplicadas (INIFTA), Facultad de Ciencias Exactas, Universidad Nacional de La Plata, C. C. 16, Suc. 4, 1900, La Plata, Argentina. E-mail: dmartire@inifta.unlp.edu.ar; Fax: +54 (0)221 4254642; Tel: +54 (0)221 4257430*
[b]*Dipartimento di Chimica, Università della Calabria, Via P., Bucci, Cubo 14 C, 87030, Arcavacata di Rende, Italy. E-mail: nrusso@unical.it; Fax: +39 0984 493390; Tel: +39-0984-492106*
[c]*Centro de Química Inorgánica (CEQUINOR, CONICET/UNLP), Facultad de Ciencias Exactas, Universidad Nacional de la Plata, C.C. 962, B1900 AVV, La Plata, Argentina*

† This article was published as part of the themed issue in honour of Esther Oliveros.

Experimental

Reagents and materials

$Na_2S_2O_8$ from Merck (Darmstadt, Germany), Waskish peat IHSS (International Humic Substances Society) HA and FA, and Aldrich humic acid sodium salt (AHA) were used as received. Distilled water (>18 MΩ cm, <20 ppb of organic carbon) was obtained from a Millipore system (Bedford, MA). The pH of the solutions employed for the flash-photolysis experiments was 3.45 ± 0.05. At this pH most of the carboxylic groups of FA are protonated. The temperature was controlled to ±0.1 K with a Grant model GD 1200 thermostat (Chelmsford, UK).

Flash-photolysis experiments

The experiments were carried out with a conventional Xenon Co. model 720C equipment (Wilmington, MA) with modified optics and electronics.[11] To avoid product accumulation, each solution was irradiated only once. Signals arising from single shots were averaged. Photolysis of $S_2O_8^{2-}$ ($\lambda_{exc} < 300$ nm) was used as a clean source of $SO_4^{\bullet-}$.[12] Data fitting was performed using Sigmaplot, which employs a Marquardt–Levenberg algorithm to determine the parameter values. The tolerance limit was set to 0.000100.

Kinetic computer simulations:

To simulate the decay of the transient traces, a computer program based on component balances formulated in terms of a differential algebraic equations system (DAE) was used. The program employs the Runge–Kutta method.[9] The method was validated by comparison with results obtained from a robust simulation of the DAE with a modified version of the LSODI routine[13] based on Gear's stiff method.[14]

TOC (total organic carbon) analysis

TOC was measured with a high-temperature carbon analyzer (Shimadzu TOC 5000 A, Kyoto, Japan).

Theoretical methodology

Molecular dynamics simulations were used as a tool to generate starting geometries for further geometry optimization with more sophisticated methods. The molecular dynamics[15] (MD) module of the *HyperChem* package[16] was used. The AM1 semiempirical method[17] was utilized to provide the potential energy in which the nuclei move. The simulation begins with a geometry that was previously optimized at the AM1 level of theory. Starting velocities were set to zero to preserve both linear and angular momenta during the whole simulation. To assure that all rotational barriers are overcome during the simulation the temperature was kept constant to a value of 500 K. The simulation time step was 0.5 fs. After an equilibration period of 10 ps, a 100-ps-long simulation was carried out, saving the coordinates every 5 ps. Those geometries were then minimized using the AM1 method. At the end of this procedure 20 starting geometries are obtained for further optimization within the framework of the density functional theory (DFT), using the ADF2007.01 package.[18] Initial optimizations were performed at the local density approximation (LDA)[19] level using a double zeta basis set available in ADF package as DZVP, which includes a set of polarization functions. The resulting four lower-energy structures were selected, on an arbitrary basis, as starting geometries for further optimization, which was performed using the PBE exchange and correlation functional[20] and a triple zeta basis set available as TZ2P, including two sets of polarization functions. This method is referred to as PBE/TZ2P hereafter. No symmetry constrains were used during geometry optimizations. We have selected the lowest-energy conformer of the Buffle model of FA and we have performed frequency calculations at the PBE/TZ2P level of theory. Different coordination modes for the interaction of the $SO_4^{\bullet-}$ and the optimized Buffle model structure were considered. Solvent effects were accounted for at a self consistent field level on the already optimized geometries. The conductor-like screening model (COSMO), using the solvent excluding surface (asurf) and the following values for the atomic radii (in Ångström), S = 1.85, O = 1.52, C = 1.70, H = 1.20 were used.[21] Reported enthalpies at 298.15 K are obtained as E° (solvent) + ΔE° (gas phase, 0 K → 298.15 K) + RT, where E° (solvent) is the total electronic energy including solvent effects self consistently on the geometry optimized in the gas phase, and ΔE° (gas phase, 0 K → 298.15 K) are the thermal corrections to the electronic energy in the gas phase obtained from the frequency calculation.

Results and discussion

Experimental results

Flash-photolysis of 0.01 M peroxodisulfate solutions without added organic substrates in the range from 289.2 to 305.2 K showed formation of $SO4^{\bullet-}$ radicals.[12]

The traces at 450 nm obtained with 0.01 M peroxodisulfate solutions in the presence of FA in the range 0–400 μg L^{-1} could be well fitted to the mixed order equation, eqn (1). Two typical traces are shown in Fig. 1.

$$A(\lambda) = \frac{k_{\text{first}}}{b(\lambda) \times \exp(k_{\text{first}} \times t) - c(\lambda)} + d(\lambda) \qquad (1)$$

$A(\lambda)$ is the time and wavelength dependent absorbance, $c(\lambda) = 2\,k_{rec}/\varepsilon(\lambda)l$ with $\varepsilon(\lambda)$ = absorption coefficient and l = optical path-length, and $b(\lambda) = c(\lambda) + k_{first}/A_o(\lambda)$ with $A_o(\lambda)$ the absorbance immediately after the lamp pulse. For experiments in the absence of FA the term $d(\lambda)$, the final constant absorption, was set = 0. For experiments in the presence of HS this term was found to be very small (less than 1% the value of $A_o(\lambda)$).

The values of k_{first} and k_{rec} obtained at 293.2 K in the absence of FA are in accordance with reported values.[6,22,23] The Arrhenius plots for k_{first} and k_{rec} yield the activation energies of (49 ± 13) and (8.4 ± 1.9) kJ mol^{-1}, respectively, in agreement with data reported by our group and by others.[6,24,25]

For fitting the data obtained in the presence of FA, the second order parameter, $c(\lambda)$ for each experiment was set equal to the value obtained from the experiment performed in the absence of FA at the same temperature.

The first order component of the $SO_4^{\bullet-}$ decay is due to reaction with the solvent, hydroxide ions, $S_2O_8^{2-}$ ions, and FA. Thus, k_{first} is in fact a pseudo first order decay rate constant. The values of k_{first} obtained at different temperatures increase with the concentration of FA expressed in μg L^{-1}, C_{FA}; as shown in Fig. 2.

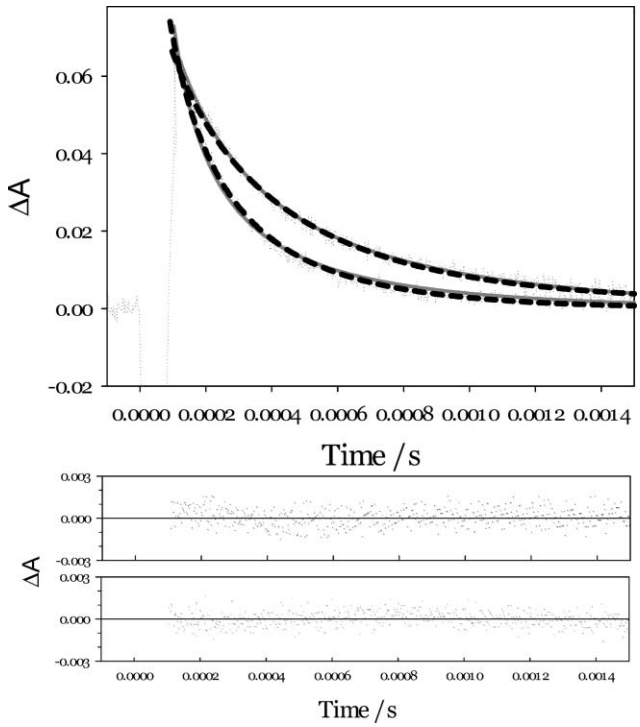

Fig. 1 Traces obtained at 450 nm with 0.01 M $Na_2S_2O_8$ solutions at 293.2 K in the absence (upper trace) and presence (lower trace) of 400 μg L^{-1} FA. The solid lines show the fitting of the data to eqn (1). The dashed lines show the computer simulations of the traces (see text). The residuals (experimental minus fitted signal) are shown below.

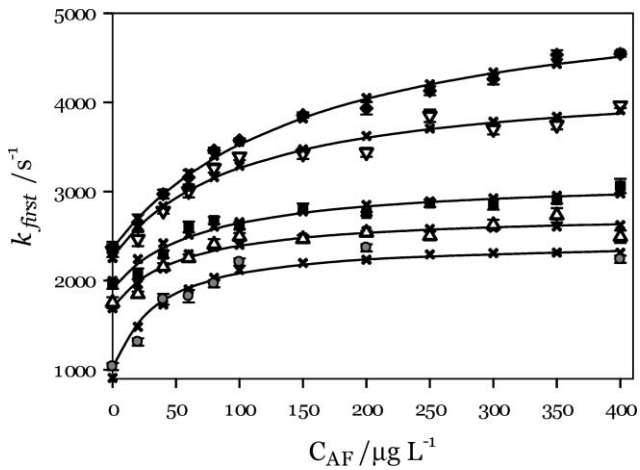

Fig. 2 Plot of k_{first} *vs.* the concentration of FA, C_{FA}, expressed in μg L^{-1}, for data obtained at different temperatures: 305.2 K (●); 301.2 K (▽); 297.2 K (■); 293.2 K (△) and 289.2 K (grey ●). The solid lines show the fitting of the data to eqn (1), and the symbols × show the values of k_{first} obtained from the fitting of the simulated traces to eqn (1) (see text).

The data shown in Fig. 2 can be fitted to eqn (2).

$$k_{first} = \frac{a + b \times C_{FA}}{1 + c \times C_{FA}} \quad (2)$$

The concentration C_{FA} is expressed in μg L^{-1}. The values of the parameters obtained at 293.2 K are: $a = (1700 \pm 90)$ s^{-1}, $b = (52 \pm 20)$ μg^{-1} L s^{-1} and $c = (0.019 \pm 0.007)$ μg^{-1} L. The concentration dependence of the data is qualitatively the same found for other HS and can be interpreted with the reactions shown in Scheme 1.[6] This kinetic analysis is based on the concentration of the molecular entities and not of the reactive sites of FA. The mechanism considers the binding of $S_2O_8^{2-}$ to FA, reaction 1. Several anions, such as chromate, arsenate, arsenite, sulfate, silicate and phosphate are known to bind to FA.[26]

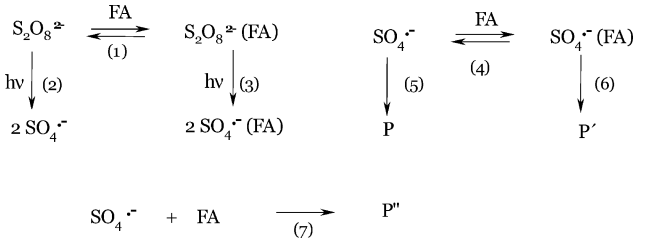

Scheme 1

Reactions (2) and (3) represent the photolysis of free and bound peroxodisulfate anion to yield free and bound $SO_4^{\bullet-}$, respectively. The rate constant k_5 is coincident with k_{first} in the absence of FA (see above). Reaction (7) occurs when $SO_4^{\bullet-}$ radicals collide with a reactive moiety of FA. P, P′ and P″ stand for reaction products.

Assuming that $SO_4^{\bullet-}$ is the main species absorbing at 450 nm and that a fast equilibrium between $SO_4^{\bullet-}$ and $SO_4^{\bullet-}$ (FA) takes place, a mixed first and second order decay is obtained for $SO_4^{\bullet-}$, as shown in eqn (3).[6]

$$-\frac{d[SO_4^{\bullet-}]}{dt} = \frac{k_{rec}[SO_4^{\bullet-}]^2 + k_5[SO_4^{\bullet-}] + k_7[SO_4^{\bullet-}][FA] + k_6 \times K_4 \times [SO_4^{\bullet-}] \times [FA]}{(1 + K_4[FA])} \quad (3)$$

Eqn (3) predicts a mixed first and second order decay kinetics for the $SO_4^{\bullet-}$ radicals with a first order rate constant, k_{first}, dependent on [FA], as shown by eqn (4).

$$k_{first} = \frac{k_5 + (k_7 + k_6 K_4)[FA]}{(1 + K_4[FA])} \quad (4)$$

The apparent first order decay rate constant, k_{first}, is given by eqn (4). The comparison of eqn (2) and (4) leads to the following values at 293.2 K: $k_5 = (1700 \pm 90)$ s^{-1}, $(k_6K_4 + k_7) = (52 \pm 20)$ μg^{-1} L s^{-1} and $K_4 = (0.019 \pm 0.007) \times 10^6 \times MW$ (with MW = average molecular weight of FA).

To further prove the proposed mechanism, computer simulations of all the experiments were performed. The experiments in the absence of FA could be reproduced by the simulation taking 6.75×10^{-6} M, for the initial concentration of $SO_4^{\bullet-}$, $[SO_4^{\bullet-}]_o$ for the experiments performed at 301.2 K, 297.2 K and 289.2 K, and 6.5×10^{-6} M for the experiments performed at 293.2 K and 305.2 K, and $\varepsilon^{450} = 1650$ $M^{-1}cm^{-1}$ for its absorption coefficient[12] and the values of both k_5 (coincident with k_{first} in the absence of FA) and k_{rec} obtained from fitting of the experimental data. There is a good agreement between the experimental and simulated traces (see upper trace in Fig. 1). Simulations of the experiments obtained in the presence of various amounts of FA were done with the same parameters employed for the simulations of the solutions without FA, taking the values of $k_6 = 5.23 \times 10^3$ s^{-1}, 4.20×10^3 s^{-1}, 3.09×10^3 s^{-1}, 2.71×10^3 s^{-1} and 2.42×10^3 s^{-1} for data at 305.2 K, 301.2 K,

297.2 K, 293.2 K and 289.2 K, respectively, and the molecular weight of 2.4×10^3 for the IHSS FA (see below), and considering the reversible steps (4) and (–4) without assuming the equilibrium condition. The contributions of the absorbance at 450 nm of both $SO_4^{\bullet-}$ and $SO_4^{\bullet-}$(FA) were considered. Simulations with different values of k_4 in the range $(1 \times 10^5 – 3 \times 10^{10})$ M^{-1} s^{-1} were performed, keeping constant the amount $K_4 = k_4/k_{-4} = c \times 10^6 \times MW$. Values of $k_4 > 1 \times 10^9$ M^{-1} s^{-1} were found to simulate well the decay traces, whereas lower values failed. Thus, a lower limit of 1×10^9 M^{-1} s^{-1} is proposed for k_4. The values of k_7 employed for the simulations, calculated as $b - k_6 \times K_4$, were 1.95×10^9 s^{-1}, 2.06×10^9 s^{-1}, 1.98×10^9 s^{-1}, 2.11×10^9 s^{-1} and 1.73×10^9 s^{-1} at 305.2 K, 301.2 K, 297.2 K, 293.2 K, and 289.2 K, respectively.

The simulated traces corresponding to experiments with various amounts of FA were fitted to the mixed order eqn (1) and the obtained k_{first} plotted against C_{FA} (crosses in Fig. 2). The values of k_{first} obtained from the simulations reproduce the saturation behavior found for the experimental values, as shown in Fig. 2 (× symbols), further supporting the proposed mechanism.

From the C content of the IHSS FA sample used here, (65 ± 2)% as determined by TOC analysis, the parameter $c = (4 \pm 1) \times 10^5$ L mol(C)$^{-1}$ at 293.2 K is obtained. From the value of the molar absorptivities of HS at 280 nm (ε), the weight-averaged molecular weight can be estimated.[27] The molecular weights calculated for the IHSS FA and for other HS are listed in Table 1. The corresponding values of the binding constants of the sulfate radicals are also listed in Table 1.

The values of K_4 for the three HS are coincident within the experimental error. From the plot of ln c *vs.* T^{-1} (Fig. 3) for the FA, the value of $\Delta H^\circ_4 = -(16 \pm 2)$ kcal mol^{-1} is obtained. From the free energy change at 298.2 K, $\Delta G^\circ_4 = -RT \ln K_4 = -10.2$ kcal mol^{-1}, and the experimental ΔH°_4, $\Delta S^\circ_4 = -20.3$ cal K^{-1} mol^{-1} is obtained. Thus, the binding of the anion is controlled by the exothermicity of the interaction.

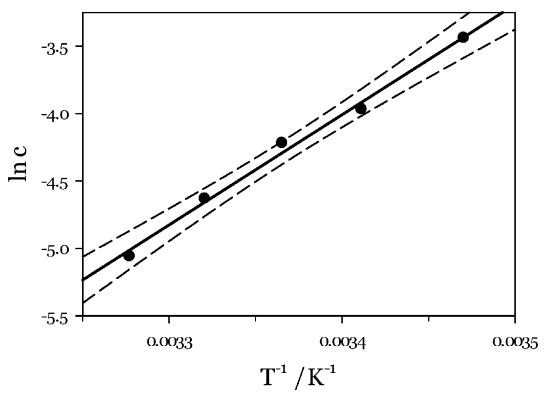

Fig. 3 Plot of ln c *vs.* T^{-1}.

Table 1 Weight-averaged molecular weights and binding constants at 293.2 K of the sulfate radicals to several HS

HS	MW/g^{-1} mol^{-1}	K_4[a,b]
IHSS FA	$(2.4 \pm 0.3) \times 10^3$[c]	$(5 \pm 3) \times 10^7$
AHA	4.1×10^3[d]	$(6 \pm 2) \times 10^7$
IHSS HA	$(2.7 \pm 0.3) \times 10^3$[c]	$(8 \pm 4) \times 10^7$

[a] K_4 was calculated as $c \times 10^6 \times$ MW. The values of c for the humic acids were taken from ref. 6 [b] The error bars in K_4 are obtained by propagating the errors in c and MW. [c] Calculated from the predictive relationship MW (g mol^{-1}) = $(4.0 \pm 0.3) \times \varepsilon$(L mol(C)$^{-1}$ cm^{-1}) + (468 ± 119) obtained by linear regression analysis of the experimental data reported in Table 1 of ref. 27 [d] From ref. 27 and 28. The error bars are not reported.

Since from the kinetic data it was possible to obtain thermodynamic information on the system, to support the proposed mechanism theoretical calculations were performed.

Theoretical results

The binding of the sulfate radicals to FA model should involve the formation of intermolecular H-bonds between both species. To check this possibility, theoretical calculations were performed using the Buffle model of FA. The optimized structure of the FA model was obtained through the procedure described in the Theoretical methodology section and is shown in Fig. 4. The structure is stabilized by the presence of five intramolecular H-bonds, as shown in the same Figure.

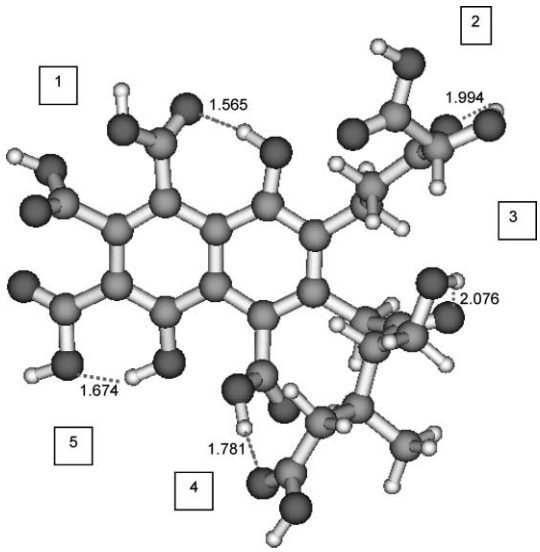

Fig. 4 PBE/TZ2P-optimized structure of the Buffle model of FA. The numbers correspond to the sites involved in the formation of the adducts shown in Fig. 5.

As previously mentioned, we have considered different coordination modes for the interaction of $SO_4^{\bullet-}$ with the FA model, and found that the lowest-energy adducts are those in which the sulfate radical is able to form two H-bonds with the Buffle model. We have therefore focused on those interaction sites and rejected higher-energy coordination modes. The favored interaction sites are shown in Fig. 4 with numbers 1 to 5. The optimized geometries of the corresponding adducts are shown in Fig. 5.

Table 2 collects the computed thermodynamic properties corresponding to the FA–$SO_4^{\bullet-}$ complexation process (reaction (4)). In particular, we report total electronic energy differences, ΔE°, that include solvent effects self-consistently. ΔH° is calculated as explained above and ΔS° is obtained from gas-phase calculations. The most stable structures are adducts 1 and 5 (Fig. 5 and Table 2), in which the sulfate radical interacts directly with ring substituents. In particular, in the most stable complex (adduct 5), the $SO_4^{\bullet-}$ radical interacts with –OH and –COOH groups, and two hydrogenic species are transferred from those groups to

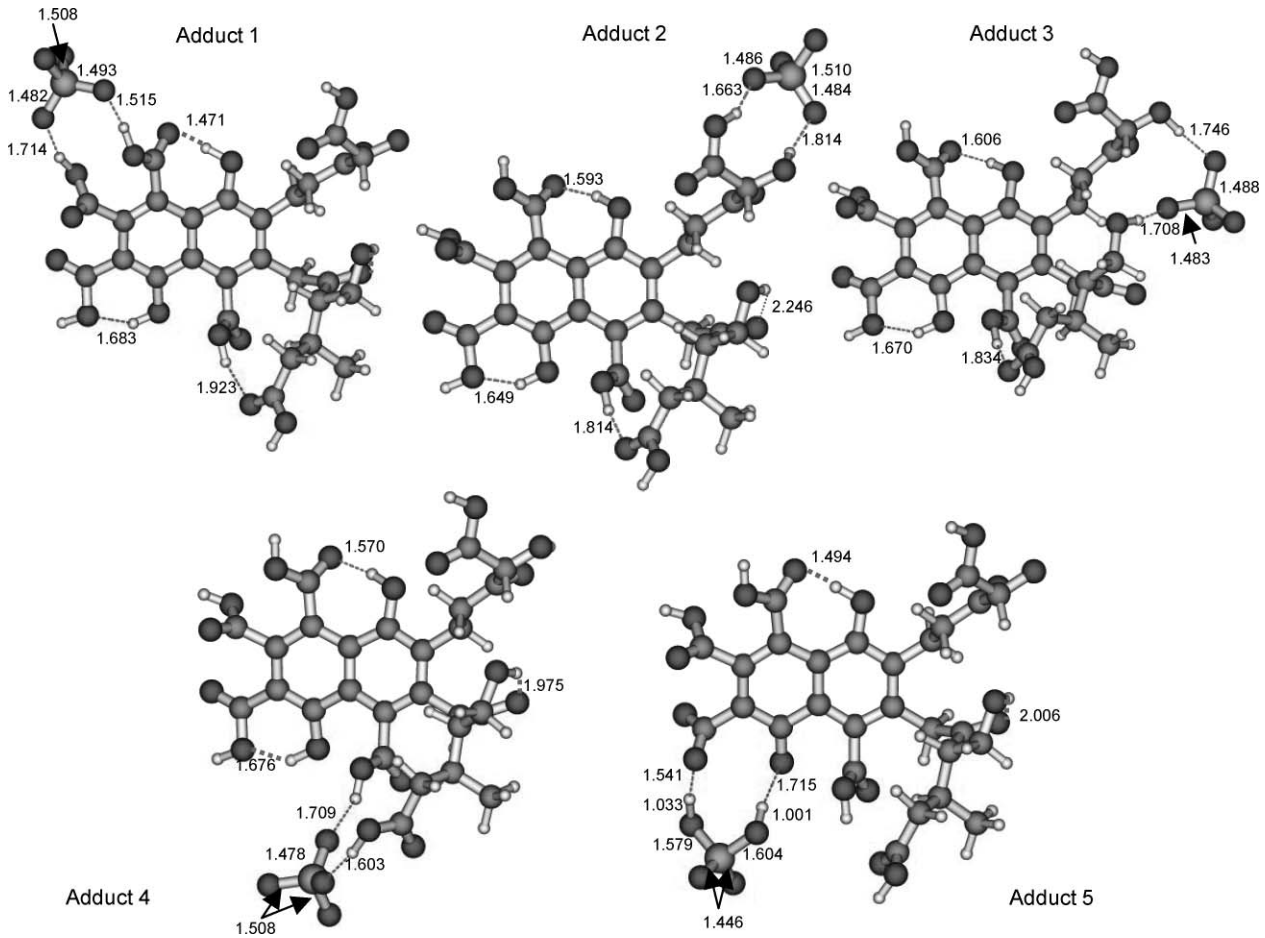

Fig. 5 PBE/TZ2P-optimized geometries of the different sulfate radical–FA adducts. Distances are in Ångström.

Table 2 Calculated (PBE/TZ2P) ΔE° for the aqueous-phase complexation reactions at 0 K, ΔH° and ΔG° values for the aqueous-phase complexation reactions at 298.15 K (all quantities are in kcal mol^{-1}); and ΔS° values for the gas-phase complexation reactions at 298.15 K in cal K^{-1} mol^{-1}

	Adduct 1	Adduct 2	Adduct 3	Adduct 4	Adduct 5
ΔE° (solvent)	–22.2	–12.5	–9.2	–13.7	–24.9
ΔH° (solvent)	–21.0	–10.9	–7.1	–11.4	–24.1
ΔS° (gas-phase)	–43.8	–41.3	–41.7	–33.5	–36.7
ΔG° (solvent)	1.5	–8.0	5.3	–1.4	–13.2

the radical. This is the only case in which we have detected such transfers. Although several additional calculations are needed to study the relative stability of adducts 1 and 5, we argue here that the transfer of two hydrogenic species, possibly a proton and a hydrogen atom, plays an important role in stabilizing adduct 5.

Our calculations indicate that ΔH° for adduct 5 at 298.15 K is –24.1 kcal mol^{-1}, whereas the corresponding ΔG° value is –13.2 kcal mol^{-1}. Adduct 1, in which the sulfate radical interacts with two –COOH groups through H-bonds is close in energy, namely, the computed ΔH° value of the complexation process was found to be –21.0 kcal mol^{-1}, whereas the corresponding ΔG° value is –8.0 kcal mol^{-1}. Our calculations also suggest that adduct 4 is only marginally stable, according to its ΔG° value, and adducts 2 and 3 are thermodynamically unstable.

Although additional calculations including solvent molecules explicitly are needed to improve the agreement between the present calculations and experimental data, some comments could be pointed out regarding those differences. The discrepancies found between empirical and calculated enthalpy and entropy changes could be understood if it is accepted that the formation of any adduct takes place in two steps. Solvation spheres are severely distorted in the first step, leading to the rupture of some of the weak solvent–molecule bonds. In the second step, both molecules with their corresponding distorted solvation spheres approach each other, then forming the adduct. The first step is clearly an endothermic process and also occurs with an increase in the system entropy. The second step, on the other hand, is an exothermic process and must occur with a decrease in the entropy of the system. In our calculations, solvation spheres are not considered explicitly or even implicitly, thus the consequences of the first step are completely ignored by the present results. In other words, more sophisticated calculations including solvent molecules explicitly should lead both to a less-exothermic enthalpy change and to a less-negative entropy change, the correct direction needed to improve present results.

Conclusion

The reaction mechanism proposed to interpret the flash-photolysis experiments requires the reversible interaction of the sulfate

radical with fulvic acids. This process was not observed in the kinetic experiments performed with gallic acid as the substrate. The presence of sites capable of forming multiple H-bonds to sulfate radicals in FA seem to stabilize it, which under such conditions "binds" to the substrate. The formation of adducts between the inorganic radicals and the Buffle model of the fulvic acids is strongly supported by the theoretical calculations. Despite the need of improving the participation of the solvent for obtaining more confident thermodynamical parameters, the trend observed in ΔH°, ΔG° and ΔS° values is in agreement with the experimental values.

The mechanism implies the competition of the contaminants and the fulvic acids for the oxidant radicals, which should lower the efficiency of the *in situ* chemical oxidation treatments involving peroxodisulfate as the oxidant. The concentration of fulvic acids dissolved in the aqueous phase during oxidative treatments could be higher than its critical micellar concentration. Under these conditions a possible adsorption process of the radicals to the fulvic acid micelles could be caused by the affinity of sulfate radicals to the fulvic acids shown in the present paper.

Acknowledgements

This research was supported by the grant PICT 2003 #14508 from Agencia Nacional de Promoción Científica y Tecnológica, (ANPCyT, Argentina), by the Italian Ministry of Foreign Affairs and the Università della Calabria. D. O. M. thanks the DAAD Alumni Program for an equipment grant. P. D. G. thanks Fundación YPF (Argentina) for a graduate studentship. M. C. G. and R. P. D. are research members of Consejo Nacional de Investigaciones Científicas y Técnicas (CONICET, Argentina). D. O. M. is a research member of Comisión de Investigaciones Científicas de la Provincia de Buenos Aires (CIC, Argentina).

References

1 A. A. Stevens, C. J. Slocum, D. R. Seeger and G. G. Robeck, Chlorination of organics in drinking water, *J. Am. Waterworks Assoc.*, 1976, **68**, 615–620.
2 T. J. Casey and K. H. Chua, Aspects of THM formation in drinking water, *J. Water Supply Res. Technol. Aqua*, 1997, **46**, 31–39.
3 J. Fu, M. Ji, Z. Wang, L. Jin and D. An, A new submerged membrane photocatalysis reactor (SMPR) for fulvic acid removal using a nano-structured photocatalyst, *J. Hazard. Mater.*, 2006, **131**, 238–242.
4 J. Fu, Y. Zhao and Q. Wu, Optimising photoelectrocatalytic oxidation of fulvic acid using response surface methodology, *J. Hazard. Mater.*, 2007, **144**, 499–505.
5 G. P. Anipsitakis and D. D. Dionysiou, Degradation of organic contaminants in water with sulfate radicals generated by the conjunction of peroxymonosulfate with cobalt, *Environ. Sci. Technol.*, 2003, **37**, 4790–4797.
6 P. M. David Gara, G. N. Bosio, M. C. Gonzalez and D. O. Mártire, Kinetics of the sulfate radical-mediated photooxidation of humic substances, *Int. J. Chem. Kinet.*, 2008, **40**, 19–24.
7 P. Caregnato, P. M. David Gara, G. N. Bosio, M. C. Gonzalez, N. Russo, M. C. Michelini and D. O. Mártire, Theoretical and experimental investigation on the oxidation of gallic aid by sulfate radical anions, *J. Phys. Chem. A*, 2008, **112**, 1188–1194.
8 P. Saparpakorn, J. H. Kim and S. Hannongbua, Investigation on the binding of polycyclic aromatic hydrocarbons with soil organic matter: A theoretical approach, *Molecules*, 2007, **12**, 703–715.
9 E. A. Nantsis and W. R. Carper, Effects of hydration on the molecular structure of magnesium–fulvic acid complexes: A MOPAC (PM3) study, *J. Mol. Struct. (THEOCHEM)*, 1999, **468**, 51–58.
10 T. de Castro Ramalho, E. F. F. da Cunha, R. Bicca de Alencastro and A. Espínola, Differential complexation between Zn^{2+} and Cd^{2+} with fulvic acid: A computational chemistry study, *Water, Air, Soil Pollut.*, 2007, **183**, 467–472.
11 M. L. Alegre, M. Geronés, J. A. Rosso, S. G. Bertolotti, A. M. Braun, D. O. Mártire and M. C. Gonzalez, Kinetic study of the reaction of chlorine atoms and $Cl_2^{\bullet-}$ radicals anions in aqueous solutions. I. Reaction with benzene, *J. Phys. Chem. A*, 2000, **104**, 3117–3125.
12 W. J. McElroy and S. J. Waygood, Kinetics of the reactions of $SO_4^{\bullet-}$ radicals with $SO_4^{\bullet-}$, $S_2O_8^{2-}$ and Fe^{+2}, *J. Chem. Soc., Faraday Trans.*, 1990, **86**, 2557–2564.
13 A. C. Hindmarsh, LSODE and LSODI two new initial value ordinary differential solvers, *ACM SIGNUM Newsletter*, 1980, **15**, 10–11.
14 A. M. Dunker, The decoupled direct method for calculating sensitivity coefficients in chemical kinetics, *J. Chem. Phys.*, 1984, **81**, 2385–2393.
15 (*a*) M. P. Allen, D. J. Tildesley, *Computer Simulation of Liquids*, Oxford University Press, Oxford, 1989; (*b*) D. C. Rapaport, *The Art of Molecular Dynamics Simulations*, Cambridge University Press, Cambridge, 2004.
16 *Hyperchem release 5.0 for Windows 1996*, Hypercube Inc., USA.
17 M. J. S. Dewar, E. G. Zoebisch, E. F. Healy and J. J. P. Stewart, Development and use of quantum mechanical molecular models. 76. AM1: A new general purpose quantum mechanical molecular model, *J. Am. Chem. Soc.*, 1985, **107**, 3902–3909.
18 (*a*) G. te Velde, F. M. Bickelhaupt, E. J. Baerends, C. Fonseca Guerra, S. J. A. van Gisbergen, J. G. Snijders and T. Ziegler, Chemistry with ADF, *J. Comput. Chem.*, 2001, **22**, 931–967; (*b*) C. Fonseca Guerra, J. G. Snijders, G. te Velde and E. Baerends, Towards an order-N DFT method, *Theor. Chem. Acc.*, 1998, **99**, 391–403; (*c*) ADF2004.01, SCM, Theoretical Chemistry, Vrije Universiteit, Amsterdam, The Netherlands, http://www.scm.com.
19 S. H. Vosko, L. Wilk and M. Nusair, Accurate spin-dependent electron liquid correlation energies for local spin density calculations: a critical analysis, *Can. J. Phys.*, 1980, **58**, 1200–1211.
20 J. P. Perdew, K. Burke and M. Ernzerhof, Generalized gradient approximation made simple, *Phys. Rev. Lett.*, 1996, **77**, 3865–3868.
21 (*a*) J. L. Pascual-Ahuir, E. Silla, J. Tomasi and R. Bonaccorsi, Electrostatic interaction of a solute with a continuum. Improved description of the cavity and of the surface cavity bound charge distribution, *J. Comput. Chem.*, 1987, **8**, 778–787; (*b*) A. Klamt and G. Schüürmann, COSMO: a new approach to dielectric screening in solvents with explicit expressions for the screening energy and its gradient, *J. Chem. Soc., Perkin Trans. 2*, 1993, 799–805; (*c*) A. Klamt, Conductor-like screening model for real solvents: A new approach to the quantitative calculation of solvation phenomena, *J. Phys. Chem.*, 1995, **99**, 2224–2235.
22 G. Bosio, S. Criado, W. Massad, F. J. Rodríguez Nieto, M. C. Gonzalez, N. A. García and D. O. Mártire, Kinetics of the interaction of sulfate and hydrogen phosphate radicals with small peptides of glycine, alanine, tyrosine, and tryptophan, *Photochem. Photobiol. Sci.*, 2005, **4**, 840–846.
23 A. B. Ross, W. G. Mallard, W. P. Helman, G. V. Buxton, R. E. Huie, P. Neta, NDRL-NIST solution kinetics database, ver. 3.0, Notre Dame Radiation Laboratory, Notre Dame, IN and National Institute of Standards and Technology, Gaithersburg, MD 1998. Available from: http://www.rcdc.nd.edu. Accessed 2009 January 15.
24 C. George and J.-M. Chovelon, A laser flash photolysis study of the decay of SO_4^- and Cl_2^- radical anions in the presence of Cl^- in aqueous solutions, *Chemosphere*, 2002, **47**, 385–393.
25 B. Ervens, *Kinetische Untersuchungen zur Atmosphärischen Chemie von $SO_4^{\bullet-}$ and $Cl_2^{\bullet-}$, Radikalanionen in Wässriger Lösung*. Diploma dissertation, Univerity of Essen, 1997.
26 S. Sachs, K. Schmeide, V. Brendler, A. Křepelová, J. Mibus, G. Geipel, T. Reich, K. H. Heise, G. Bernhard, in *Investigations on the Complexation Behaviour of Humic Acids and their Influence on the Migration of Radioactive and Non-Radioactive Substances under Conditions Close to Nature*, ed. C. M. Marquardt, Forschungszentrum Karlsruhe GmbH, Karlsruhe, Germany, 2004, pp. 19-94.
27 Y.-P. Chin, G. Aiken and E. O'Loughlin, Molecular weight, polydispersity, and spectroscopic properties of aquatic humic substances, *Environ. Sci. Technol.*, 1994, **28**, 1853–1858.
28 I. V. Perminova, F. H. Frimmel, A. V. Kudryavtsev, N. A. Kulikova, G. Abbt-Braun, S. Hesse and V. S. Petrosyan, *Environ. Sci. Technol.*, 2003, **37**, 2477–2485.